

OPTIMISATION PROCEDURE FOR PARAMETER IDENTIFICATION IN INELASTIC MATERIAL INDENTATION TESTING*

DAN DUMITRIU¹, GASTON RAUCHS², VETURIA CHIROIU¹

The indentation of an inelastic material isotropic half-space with a spherical tip indenter is simulated using an in-house finite element code written in Fortran. In order to identify seven unknown material parameters (E and ν for elasticity; $\sigma^{y,0}$, R , β , H_{kin} and H_{nl} for plasticity), the simulation results must match as good as possible the experimental load-penetration curve obtained when indenting the inelastic material. This material parameter identification is performed using an optimisation procedure, *i.e.*, one has to minimize the difference between the experimental curve and the simulated one. The optimisation procedure used here starts by applying a Gauss-Newton method, then continues using a Levenberg-Marquardt method. Using this optimisation procedure, the material parameter identification was successfully achieved for the considered indentation case study.

1. INTRODUCTION

This paper deals with the parameter identification in indentation testing of inelastic materials. It is an inverse engineering problem very relevant to industry, the purpose being to determine one or more inelastic material parameters that would lead to the most accurate agreement between experimental data and indentation simulation results. Since indentation modelling involves non-uniform stress fields to be analysed and non-linear material behaviour, there is no straightforward analytical solution for material parameter identification associated to indentation testing. So, numerical approaches – finite element modelling in this case – must be used for obtaining the fields of the state variables corresponding to the indentation test.

Suppose one has to determine the unknown parameters of a new inelastic material. Using a nanoindenter, experimental load-penetration curves are available for the new, unknown material. Based on this experimental data, the purpose is to identify the unknown material parameters: Young's modulus E and Poisson's ratio ν (elasticity parameters), respectively the initial uniaxial yield stress $\sigma^{y,0}$, the non-linear isotropic hardening parameters R and β and the non-linear kinematic

*Presented at SISOM2007 and Homagial Session of the Commission of Acoustics, Bucharest, 29–31 May 2007.

¹ Institute of Solid Mechanics, Romanian Academy, Bucharest, Romania

² Laboratoire de Technologies Industrielles, Centre de Recherche Public Henri Tudor, Grand Duchy of Luxembourg, Corresponding author: D. Dumitriu, Address: Str. Ctin Mille nr. 15, Sector 1, 010141 Bucharest, Romania, Fax: +40 21 3126736, Email: dumitri04@yahoo.com

hardening parameters H_{kin} si H_{nl} (plasticity parameters). In what concerns the simulation of the indentation, an in-house FEM code for finite elasto-plastic strains called SPPRc is used. This software implements the stress update equations and models the contact between the spherical tip indenter and the unknown inelastic material [1]. The stress update equations are formulated based on the constitutive equations for hypo-elastic material behaviour and considering associative plasticity with isotropic J2-flow theory. Using SPPRc software and initializing the seven unknown parameters with initial guesses in the range between some lower and upper bounds, an optimisation procedure is launched in order to minimize the objective function, *i.e.*, the difference or gap between the experimental load-penetration curve and the simulated one.

So, by means of the optimization procedure, the material parameters are updated until the minimization of the objective function is achieved. Several approaches are available for this optimization procedure, from classical gradient-based numerical optimization to modern neural networks approach. Gradient-based numerical optimization methods [5] were preferred here, knowing that neural networks need a big amount of objective function evaluations and here the computational time for one evaluation is not negligible. Ponthot and Kleiner mann [2] proposed to solve parameter identification inverse problems using a cascade optimization methodology, *i.e.*, a robust and efficient sequence of gradient-based optimization methods. The optimization procedure proposed here is a sequence of two gradient-based optimization methods, *i.e.*, the Gauss-Newton method and the Levenberg-Marquardt method. The gradient of the objective function, *i.e.*, the vector of the objective function derivatives with respect to the unknown parameters, is computed in a sensitivity analysis, using the direct differentiation method to calculate the derivatives of the state variables with respect to the material parameters. This direct differentiation method calculates directly the derivatives, through an incremental linear update scheme during the incremental solution of the direct deformation problem [1]. The computational effort is thus considerably reduced, compared with the numerical calculation of the derivatives by finite differences.

2. THE MATERIAL BEHAVIOUR: CONSTITUTIVE AND STRESS UPDATE EQUATIONS

Associative plasticity with isotropic J2-flow theory is considered [1]. Plastic yielding is governed by the yield function f :

$$f = \|\mathbf{P} : (\boldsymbol{\sigma} - \boldsymbol{\alpha})\| - K^y \quad \begin{cases} f < 0 & \text{for elastic material behavior,} \\ f = 0 & \text{for plastic material behavior,} \\ f > 0 & \text{excluded,} \end{cases} \quad (1)$$

where K^y is the yield limit, $\boldsymbol{\alpha}$ the back-stress, an internal variable, $\boldsymbol{\sigma}$ is the Cauchy stress and \mathbf{P} is the deviatoric projection operator

$$\mathbf{P} = \mathbf{I}^S - \frac{1}{3} \mathbf{I} \otimes \mathbf{I},$$

where \mathbf{I}^S is the fourth-order symmetric identity tensor. The variation of the yield limit K^y is described through isotropic hardening, with [1]:

$$K^y = \sqrt{\frac{2}{3}} \left\{ \sigma^{y,0} + \frac{R}{\beta} [1 - \exp(-\beta s)] \right\}, \quad (3)$$

where s is the plastic arc length, $\sigma^{y,0}$ is the initial uniaxial yield stress, and R and β are the non-linear isotropic hardening parameters. For kinematic hardening, the Armstrong-Frederick law with the non-linear kinematic hardening parameters H_{kin} and H_{nl} is considered:

$$\dot{\boldsymbol{\alpha}} = H_{\text{kin}} \dot{\boldsymbol{\varepsilon}}^p - \sqrt{\frac{2}{3}} H_{\text{nl}} \dot{s} \boldsymbol{\alpha}. \quad (4)$$

The hypo-elastic material behaviour is described using Hooke's law, relating the Cauchy stress $\boldsymbol{\sigma}$ to the elastic strains $\boldsymbol{\varepsilon}^{\text{el}}$ through the Lamé constants G and λ :

$$\boldsymbol{\sigma} = (2G \mathbf{I}^S + \lambda \mathbf{I} \otimes \mathbf{I}) : \boldsymbol{\varepsilon}^{\text{el}} = \mathbf{C} : \boldsymbol{\varepsilon}^{\text{el}}, \quad (5)$$

where \mathbf{C} is the corresponding fourth-order tensor.

Based on the constitutive equations above, the stress update equations can now be formulated. The state variables at the beginning of an increment are characterized by a superscript 0 , whereas those at the end of the increment are characterized by a superscript 1 , and the mid-step configurations are characterized by a superscript ${}^{1/2}$. In the finite strain case, rigid body rotation is accounted for to preserve material objectivity, henceforth a corotational formulation is used in order to transform all tensor-valued state variables into the same rotation-neutralized coordinate frame.

In this rotation-neutralized coordinate frame, the classical update scheme of the plastic arc length s , of the plastic strain $\boldsymbol{\varepsilon}^p$, of the stress $\boldsymbol{\sigma}$ and of the back-stress $\boldsymbol{\alpha}$ is [1]:

$$s^1 = s^0 + \sqrt{\frac{2}{3}} \Delta g, \quad (6)$$

$$\hat{\boldsymbol{\varepsilon}}^{\text{p},1} = \hat{\boldsymbol{\varepsilon}}^{\text{p},0} + \Delta g \hat{\mathbf{N}}^1, \quad (7)$$

$$\hat{\boldsymbol{\sigma}}^1 = \hat{\boldsymbol{\sigma}}^0 + \mathbf{C} : \Delta \hat{\boldsymbol{\varepsilon}}^{1/2} - 2G \Delta g \hat{\mathbf{N}}^1, \quad (8)$$

$$\hat{\boldsymbol{\alpha}}^1 = \exp(-H_{\text{nl}} \Delta g) \hat{\boldsymbol{\alpha}}^0 + [1 - \exp(-H_{\text{nl}} \Delta g)] \frac{H_{\text{kin}}}{H_{\text{nl}}} \hat{\mathbf{N}}^1, \quad (9)$$

with the total strain increment $\Delta\hat{\boldsymbol{\varepsilon}}^{1/2}$ calculated according to the midpoint-rule, and the normalized tensor $\hat{\mathbf{N}}^1$ defined by:

$$\hat{\mathbf{N}}^1 = \frac{\hat{\mathbf{P}}^1 : (\hat{\boldsymbol{\sigma}}^1 - \hat{\boldsymbol{\alpha}}^1)}{\|\hat{\mathbf{P}}^1 : (\hat{\boldsymbol{\sigma}}^1 - \hat{\boldsymbol{\alpha}}^1)\|} = \frac{\hat{\mathbf{P}}^1 : (\hat{\boldsymbol{\sigma}}^1 - \hat{\boldsymbol{\alpha}}^1)}{K^y}. \quad (10)$$

The plastic consistency parameter Δg is obtained from the equation expressing the yield function (1) for plastic material behaviour:

$$f = \|\mathbf{P} : \hat{\boldsymbol{\sigma}}^0 + 2G\mathbf{P} : \Delta\hat{\boldsymbol{\varepsilon}}^{1/2} - \exp(-H_{nl}\Delta g)\hat{\boldsymbol{\alpha}}^0\| - 2G\Delta g - \frac{H_{kin}}{H_{nl}}[1 - \exp(-H_{nl}\Delta g)] - K^y = 0. \quad (11)$$

A local Newton-Raphson scheme is used to determine Δg from (11).

3. UNIAXIAL INDENTATION TEST

The uniaxial indentation test consists in pushing a hard indenter vertically into the plane surface of the material specimen (Fig. 1a). A nanoindenter can record the load P and the penetration h_{tip} of the indenter tip into the surface, where the penetration h_{tip} is the total displacement of the specimen contact surface at the vertical line of symmetry. The spherical tip of the indenter has hypo-elastic material behaviour, with Young's modulus $E_{tip} = 1016$ GPa and Poisson's ratio $\nu_{tip} = 0.07$.

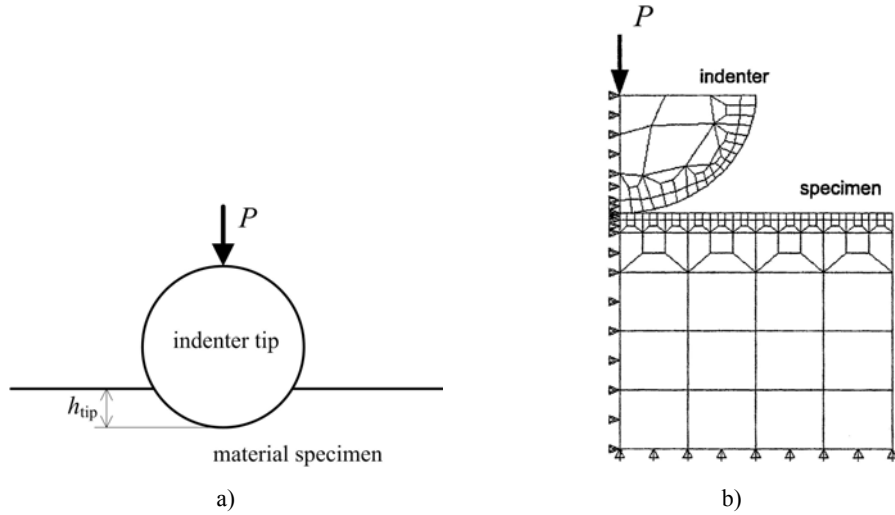


Fig. 1 – a) Scheme of the uniaxial indentation test;
b) axisymmetric finite element model of the indentation test [1].

In this inelastic material indentation problem, the parameter identification concerns seven unknown material parameters: Young's modulus E and Poisson's ratio ν (elasticity parameters), respectively the initial uniaxial yield stress $\sigma^{y,0}$, the non-linear isotropic hardening parameters R and β and the non-linear kinematic hardening parameters H_{kin} si H_{nl} (plasticity parameters). In fact, the linear hardening parameters R and H_{kin} have been replaced with the following parameters, which both have the physical meaning of a stress:

$$H_{\text{kin}}^* = \frac{H_{\text{kin}}}{H_{\text{nl}}} \quad \text{and} \quad R^* = \frac{R}{\beta}. \quad (12)$$

The axisymmetric finite element model for spherical indenter tip and material specimen is shown in Fig. 1b, where 112 bi-quadratic elements were used to model half of the material specimen and 47 bi-quadratic elements were used to model half of the spherical tip indenter. The simulations are performed using SPPRc which implements the stress update equations (6)–(9) for this axisymmetric finite element model, considering finite elasto-plastic strains.

In SPPRc, the contact modelling between the indenter tip and the material specimen is realized by inhibiting the geometrical interpenetration of the two bodies. This can be achieved by applying tractions over the contact area. The surface of the indenter is the master surface, whereas the nodes on the material specimen surface are the slave nodes. In simple contact formulations like penalty or augmented logarithmic barrier methods, the tractions to be applied on the contact boundary for inhibiting interpenetration are calculated from the local gap between slave nodes and their projection on the master segment. More details about the contact modelling can be found in [1].

The indentation test considered here is in fact a virtual indentation test, the purpose being mainly to validate the proposed material parameter identification optimization procedure. More precisely, a simulation of the indentation test is carried out with known material parameters, and the resulting load-penetration curve (see Fig. 2) is used as artificial experimental data, called also pseudo-experimental data. The material parameters used to obtain the pseudo-experimental data are given in Table 1. The parameter identification optimization procedure is then started with a different set of material parameters, a virtual initial guess, and should ideally converge to the material parameters used to obtain the pseudo-experimental data.

Table 1

Material parameters used in the artificial experiment

	E [MPa]	ν	$\sigma^{y,0}$ [MPa]	R^* [MPa]	β	H_{kin}^* [MPa]	H_{nl}
Artificial experiment	200000	0.3	400	100	100	200	50

The artificial, pseudo-experimental load-penetration curve considered in this paper concerns only a single load-unload cycle (see Fig. 2). Of course, more complex cycles can be considered, *e.g.*, load-unload-reload-load-unload cycle, also residual imprint mapping data can be taken into consideration.

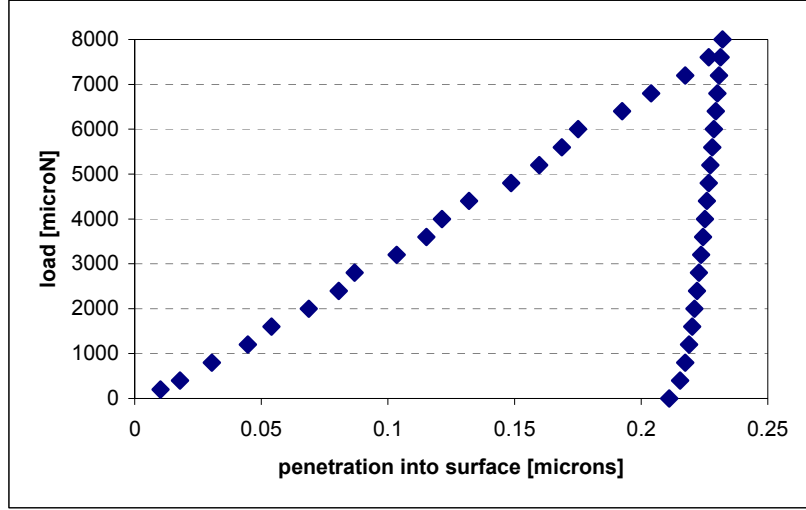


Fig. 2 – Artificial, pseudo-experimental load-penetration curve for single load-unload cycle.

4. PARAMETER IDENTIFICATION OPTIMIZATION PROCEDURE

Let \mathbf{x} denote the vector of the seven material parameters to be identified:

$$\mathbf{x} = [E \quad \nu \quad \sigma^{y,0} \quad R^* \quad \beta \quad H_{\text{kin}}^* \quad H_{\text{nl}}]^T. \quad (13)$$

The material parameter identification is performed using an optimization procedure, *i.e.*, one has to minimize (bring to zero, if possible) the difference between the simulated curve and the pseudo-experimental one. Both load-penetration curve and residual imprint mapping data are considered for comparing simulation with pseudo-experimental results. The objective function to be minimized is thus:

$$\Xi = \sum_{k=1}^N [h_{\text{tip}}^{\text{sim}}(P^k) - h_{\text{tip}}^{\text{exp}}(P^k)]^2 + \sum_{l=1}^{N^*} \{[u^{\text{sim}}(\mathbf{r}^l) - u^{\text{sim}}(\mathbf{r}^0)] - [u^{\text{exp}}(\mathbf{r}^l) - u^{\text{exp}}(\mathbf{r}^0)]\}^2, \quad (14)$$

with:

- N – the number of points in which simulated and pseudo-experimental penetrations are compared;

- $h_{\text{tip}}^{\text{sim}}(P^k)$ – the simulated penetration of the indenter tip into the surface corresponding to the load P^k at time t^k , using the material parameters computed at that stage of the optimization procedure;
- $h_{\text{tip}}^{\text{exp}}(P^k)$ – pseudo-experimental penetration corresponding to load P^k ;
- N^* – number of fixed radial locations \mathbf{r}^l where simulated and pseudo-experimental residual imprints are compared;
- $u^{\text{sim}}(\mathbf{r}^l)$ – the simulated total vertical displacement at the fixed radial location \mathbf{r}^l ;
- $u^{\text{sim}}(\mathbf{r}^0)$ – simulated total vertical displacement at the reference point \mathbf{r}^0 , *e.g.*, the imprint centre;
- $u^{\text{exp}}(\mathbf{r}^l)$ – pseudo-experimental total vertical displacement at the fixed radial location \mathbf{r}^l ;
- $u^{\text{exp}}(\mathbf{r}^0)$ – pseudo-experimental total vertical displacement at the reference point \mathbf{r}^0 .

The gradient of the objective function Ξ with respect to the variables vector \mathbf{x} is:

$$\begin{aligned} \nabla \Xi &= \left[\frac{\partial \Xi}{\partial x_1} \quad \frac{\partial \Xi}{\partial x_2} \quad \frac{\partial \Xi}{\partial x_3} \quad \frac{\partial \Xi}{\partial x_4} \quad \frac{\partial \Xi}{\partial x_5} \quad \frac{\partial \Xi}{\partial x_6} \quad \frac{\partial \Xi}{\partial x_7} \right]^T = \\ &= \left[\frac{\partial \Xi}{\partial E} \quad \frac{\partial \Xi}{\partial \nu} \quad \frac{\partial \Xi}{\partial \sigma^{y,0}} \quad \frac{\partial \Xi}{\partial R^*} \quad \frac{\partial \Xi}{\partial \beta} \quad \frac{\partial \Xi}{\partial H_{\text{kin}}^*} \quad \frac{\partial \Xi}{\partial H_{\text{nl}}} \right]^T, \end{aligned} \quad (15)$$

where the derivative of the objective function Ξ with respect to the material parameter x_i ($i = 1, \dots, 7$) follows from (14):

$$\begin{aligned} \frac{\partial \Xi}{\partial x_i} &= 2 \sum_{k=1}^N \left[h_{\text{tip}}^{\text{sim}}(P^k) - h_{\text{tip}}^{\text{exp}}(P^k) \right] \frac{\partial h_{\text{tip}}^{\text{sim}}(P^k)}{\partial x_i} + \\ &+ 2 \sum_{l=1}^{N^*} \left\{ [u^{\text{sim}}(\mathbf{r}^l) - u^{\text{sim}}(\mathbf{r}^0)] - [u^{\text{exp}}(\mathbf{r}^l) - u^{\text{exp}}(\mathbf{r}^0)] \right\} \frac{\partial [u^{\text{sim}}(\mathbf{r}^l) - u^{\text{sim}}(\mathbf{r}^0)]}{\partial x_i}. \end{aligned} \quad (16)$$

As for the derivatives $\frac{\partial h_{\text{tip}}^{\text{sim}}(P^k)}{\partial x_i}$ and $\frac{\partial [u^{\text{sim}}(\mathbf{r}^l) - u^{\text{sim}}(\mathbf{r}^0)]}{\partial x_i}$, they are computed

from the derivatives of the state variables with respect to the material parameter x_i . The direct differentiation method is used to perform this sensitivity analysis as

described in [1]. The elements H_{ij} of the Hessian matrix \mathbf{H} , *i.e.*, the second order derivatives $\frac{\partial^2 \Xi}{\partial x_i \partial x_j}$, can be deduced by deriving (16):

$$\begin{aligned}
H_{ij} = \frac{\partial^2 \Xi}{\partial x_i \partial x_j} = & 2 \sum_{k=1}^N \left\{ \frac{\partial h_{\text{tip}}^{\text{sim}}(P^k)}{\partial x_i} \frac{\partial h_{\text{tip}}^{\text{sim}}(P^k)}{\partial x_j} + [h_{\text{tip}}^{\text{sim}}(P^k) - h_{\text{tip}}^{\text{exp}}(P^k)] \frac{\partial^2 h_{\text{tip}}^{\text{sim}}(P^k)}{\partial x_i \partial x_j} \right\} \\
& + 2 \sum_{l=1}^{N^*} \left\{ \frac{\partial [u^{\text{sim}}(\mathbf{r}^l) - u^{\text{sim}}(\mathbf{r}^0)]}{\partial x_i} \frac{\partial [u^{\text{sim}}(\mathbf{r}^l) - u^{\text{sim}}(\mathbf{r}^0)]}{\partial x_j} + \right. \\
& \left. + [(u^{\text{sim}}(\mathbf{r}^l) - u^{\text{sim}}(\mathbf{r}^0)) - (u^{\text{exp}}(\mathbf{r}^l) - u^{\text{exp}}(\mathbf{r}^0))] \frac{\partial^2 [u^{\text{sim}}(\mathbf{r}^l) - u^{\text{sim}}(\mathbf{r}^0)]}{\partial x_i \partial x_j} \right\}. \tag{17}
\end{aligned}$$

The optimization procedure proposed in this paper is a sequence of two gradient-based optimization methods, *i.e.*, the Gauss-Newton method and the Levenberg-Marquardt method. The optimization problem here is a minimization with simple bounds, *i.e.*, the variables of the minimization problem are limited by constant lower and upper bounds.

The Gauss-Newton optimization method is an iterative method based on the following recurrence relation [4]–[5]:

$$\mathbf{x}^{p+1} = \mathbf{x}^p - \mu^p [\mathbf{H}^p]^{-1} (\nabla \Xi)^p, \tag{18}$$

where p denotes here the iteration number and μ^p is the parameter of the line search algorithm performed inside the Gauss-Newton method to find the lowest value of the objective function Ξ along the search direction $[\mathbf{H}^p]^{-1} (\nabla \Xi)^p$. The Hessian matrix \mathbf{H}^p given by (17) has to be positive definite in order to provide that the search direction is a descent direction [3], *i.e.*, in order to converge towards a minimum of the objective function.

As for the Levenberg-Marquardt optimization method [3]–[5], its recurrence relation is:

$$\mathbf{x}^{p+1} = \mathbf{x}^p - [(\mathbf{J}^p)^T \mathbf{J}^p + \xi^p \mathbf{I}]^{-1} (\mathbf{J}^p)^T \Xi^p, \tag{19}$$

where \mathbf{J} is the Jacobian defined here as

$$\mathbf{J} = \begin{bmatrix} \frac{\partial \Xi}{\partial E} & \frac{\partial \Xi}{\partial v} & \frac{\partial \Xi}{\partial \sigma^{y,0}} & \frac{\partial \Xi}{\partial R^*} & \frac{\partial \Xi}{\partial \beta} & \frac{\partial \Xi}{\partial H_{\text{kin}}^*} & \frac{\partial \Xi}{\partial H_{\text{nl}}} \end{bmatrix} = (\nabla \Xi)^T, \tag{20}$$

and where the scalar ξ^p is determined as follows:

$$\xi^p = 10^{-15}$$

$$\text{DO } \xi^p = 10 \cdot \xi^p \quad (21)$$

UNTIL matrix $[(\mathbf{J}^p)^T \mathbf{J}^p + \xi^p \mathbf{I}]$ becomes positive definite.

The implementation in SPPRc software of the Gauss-Newton and Levenberg-Marquardt methods was done by means of the respective subroutines provided by IMSL Fortran Math Library [4].

5. CONVERGENCE RESULTS

The parameter identification optimization procedure proposed in §4 was applied to the virtual uniaxial indentation problem described in §3. The pseudo-experimental load-penetration curve is the one shown previously in Fig. 2, where only a single load-unload cycle has been considered. The residual imprint mapping data taken into account in provided in Table 2, with the reference point located on the vertical symmetry axis, *i.e.*, $\mathbf{r}^0 = 0$.

Table 2

Residual imprint mapping data

index l	1	2	3	4	5	6	7	8	9
\mathbf{r}^l [μm]	0.125	0.250	0.375	0.500	0.625	0.750	0.875	1.000	1.125
$u^{\text{exp}}(\mathbf{r}^l) - u^{\text{exp}}(\mathbf{r}^0)$ [μm]	0.003 5	0.012 7	0.027 9	0.049 5	0.077 5	0.112 1	0.153 6	0.201 9	0.246 2

10	11	12	13	14	15	16	17	18	19	20
1.250	1.375	1.500	1.625	1.750	1.875	2.000	2.125	2.250	2.375	2.500
0.238 3	0.231 4	0.226 5	0.223 1	0.220 5	0.218 5	0.216 8	0.215 6	0.214 6	0.213 8	0.213 2

Starting from various virtual initial guesses, the optimisation procedure proposed in §4 is supposed to converge to the material parameters used to obtain the pseudo-experimental data, *i.e.*, the ones in Table 1. Two such convergence tests T1 and T2 were performed, Table 3 presenting the virtual initial guesses used in these two tests, as well as the lower and upper bounds of the seven parameters to be identified, plus the solution of the problem, *i.e.*, the pseudo-experimental material parameters from Table 1.

Table 3

Different values for the material parameters:
T1 and T2 initial guesses, upper and lower bounds, problem's solution

	E [MPa]	ν	$\sigma^{y,0}$ [MPa]	R^* [MPa]	β	H_{kin}^* [MPa]	H_{nl}
T1 initial guesses	100000	0.2	800	50	200	50	100
T2 initial guesses	261110	0.34	667	46	523	398	74
Artificial experiment	200000	0.3	400	100	100	200	50
Lower bounds	30000	0.05	1	0	10	0	10
Upper bounds	600000	0.49	1000	1000	1500	1000	1500

The proposed optimisation procedure consists in a sequence of four stages:

- Gauss-Newton method (18) applied on variables E and $\sigma^{y,0}$, the other variables being blocked on their initial guesses (called G-N1, maximum 8 iterations allowed);
- Gauss-Newton method (18) applied on all seven variables (called G-N2, maximum 10 iterations);
- Levenberg-Marquardt method (19) applied on three variables (the variables located temporarily on the bounds, then the variables x_i corresponding to the smallest $\frac{\partial \Xi}{\partial x_i}$), the other four variables being blocked on their previous values (called L-M1, maximum 15 iterations allowed);
- Levenberg-Marquardt method (19) applied on all seven variables (called L-M2, maximum 30 iterations allowed).

Fig. 3a shows the convergence of the optimisation procedure for the first numerical test T1, where the objective function is minimized up to $\Xi_{\min,T1} = 1.28 \cdot 10^{-12} \mu\text{m}^2$. Fig. 3b shows the convergence results for the second numerical test T2, where the objective function is minimized up to $\Xi_{\min,T2} = 7.16 \cdot 10^{-9} \mu\text{m}^2$. Both figures show the reduction of $\log_{10} \Xi$ with the number of iterations performed. The vertical dotted lines indicate the switches between the four stages of the optimisation procedure.

The results are satisfactory, showing the reliability of the proposed four stages optimisation procedure, based on Gauss-Newton and Levenberg-Marquardt methods. The objective function is always decreasing for both tests presented, without diverging or blocking in undesired local minima. The objective function has been practically brought to zero, the material parameters obtained by this identification procedure matching almost perfectly the considered pseudo-experimental material parameters.

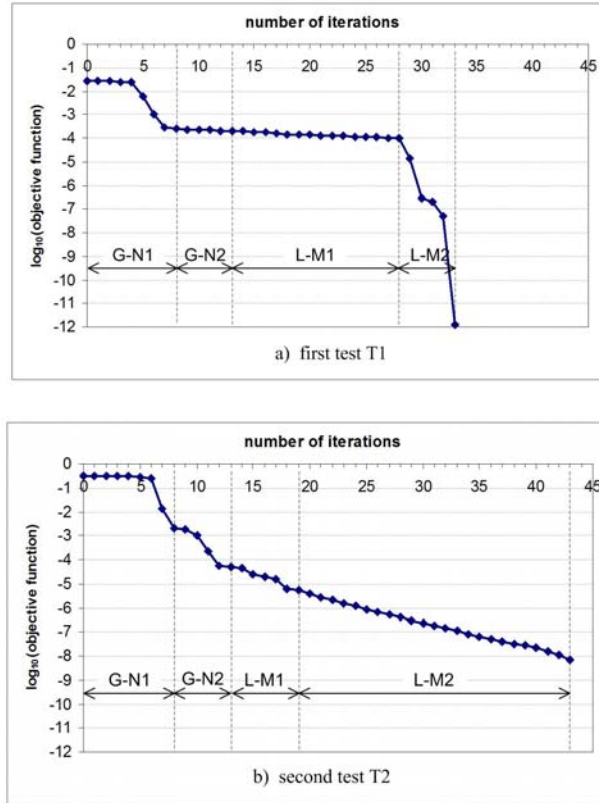


Fig. 3 – Reduction of $\log_{10} \Xi$ with the number of iterations for: a) first test T1; b) second test T2.

6. CONCLUSIONS

The framework of this work is the parameter identification related to inelastic material indentation testing. The goal of this inverse problem is to determine the unknown material parameters of a specimen, in order to reach some experimental data measured on that specimen.

More precisely, the purpose of this paper was to propose a reliable variant of optimization procedure for this material parameter identification problem. Based on IMSL Fortran Math Library [4] subroutines, the optimization procedure was implemented in SPPRC, an in-house FEM software for finite elasto-plastic strains. The optimization procedure was divided in four stages, two stages based on Gauss-Newton method, followed by two stages based on Levenberg-Marquardt method. The convergence results towards the desired global minimum were satisfactory. Further investigations, including additional load cycles of the indentation test, are

necessary in order to increase and guarantee the reliability of this parameter identification optimization procedure.

Gradient-based optimization methods, such as Gauss-Newton and Levenberg-Marquardt methods, are local optimizers, bearing the necessity to supply an appropriate initial guess, in order to place the optimization problem closer to its searched global optimum. So, further work may provide a more elaborated initialization of the unknown material parameters, not just a simple guess.

Acknowledgements. Gaston RAUCHS gratefully acknowledges the financial support of the Fonds National de la Recherche (FNR) of the Grand Duchy of Luxembourg, through grant number FNR-05/02/01-VEIANEN.

Dan DUMITRIU and Veturia CHIROIU gratefully acknowledge the financial support of the National Authority for Scientific Research Council (ANCS), Romania, through CEEX postdoctoral grant nr. 1531/2006, which funded the visit of Dan DUMITRIU at the Centre de Recherche Public Henri Tudor.

REFERENCES

1. RAUCHS, G., *Optimization-based material parameter identification in indentation testing for finite strain elasto-plasticity*, ZAMM – Z. Angew. Math. Mech., **86**, 7, pp. 539–562 (2006).
2. PONTHOT, J.-P., KLEINERMANN, J.-P., *A cascade optimization methodology for automatic parameter identification and shape/process optimization in metal forming simulation*, Comput. Methods Appl. Mech. Engrg., **195**, pp. 5472–5508 (2006).
3. SEIFERT, T., SCHENK, T., SCHMIDT, I., *Efficient and modular algorithms in modeling finite inelastic deformations: Objective integration, parameter identification and sub-stepping techniques*, Comput. Methods Appl. Mech. Engrg., **196**, pp. 2269–2283 (2007).
4. *IMSL Math/Library vol. 1 and 2 – FORTRAN Subroutines for Mathematical Applications*, Visual Numerics, Inc., pp. 867–1029 (Chapter 8: “Optimization”), 1997.
5. NOCEDAL, J., WRIGHT, S.J., *Numerical Optimization*, Springer Verlag, New York, 1999.